Title
Hydrogenated Amorphous Silicon Pixel Detectors for Minimum Ionizing Particles

Journal
Nuclear Instruments and Methods in Physics Research A, 273

Authors
Perez-Mendez, V.
Kaplan, S.N.
Cho, G.
et al.

Publication Date
1988-04-01

LBL-25114 c.1
Preprint

Lawrence Berkeley Laboratory
UNIVERSITY OF CALIFORNIA

Physics Division

Submitted to Nuclear Instruments and Methods in Physics Research

Hydrogenated Amorphous Silicon Pixel Detectors for Minimum Ionizing Particles

V. Perez-Mendez, S.N. Kaplan, G. Cho, I. Fujieda,
S. Qureshi, W. Ward, and R.A. Street

April 1988

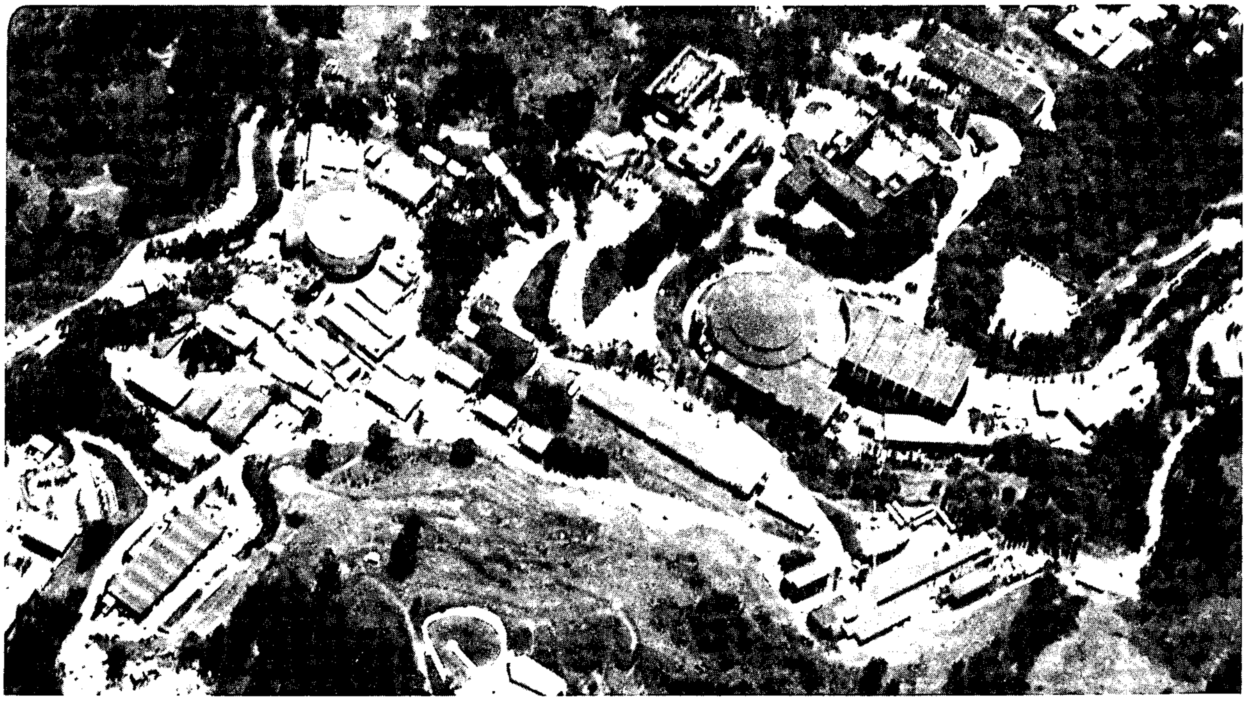

Prepared for the U.S. Department of Energy under Contract Number DE-AC03-76SF00098.

Submitted to N.I.M.

LBL-25114
April 1988

Hydrogenated Amorphous Silicon Pixel Detectors for Minimum Ionizing Particles

V. Perez-Mendez, S. N. Kaplan, G. Cho, I. Fujieda, S. Qureshi, W. Ward
Lawrence Berkeley Laboratory, Berkeley, CA

R. A. Street
Xerox Palo Alto Research Center, Palo Alto, CA

I. Introduction

Various design parameters for present and future colliding beam accelerators include position-sensitive pixel arrays both in tracking devices and in calorimeters using scintillation detectors. The need for pixel detectors—arrays in which each position-sensitive element is addressed individually by its own amplifier-logic electronics—arises from the anticipated event rate and the need to eliminate x,y ambiguities in multi-track events that would arise if the more conventional x,y strip multiplexing is used. Many of these detectors propose the use of xtal silicon pixels connected to integrated circuit (xtal Si) amplifier read-out logic.(1) Since a-Si:H detectors are intrinsically capable of being constructed in large areas, by techniques similar to those used in the solar cell industry, and since thin-film a-Si:H FET-are readily made by the same deposition techniques, this combination offers a potentially useful alternative to xtal Si diode detectors and various gas-filled devices. In this paper we report on measurement of minimum ionizing particles with hydrogenated amorphous silicon (a-Si:H) detectors having thicknesses and sensitivities that should already be sufficient for use in such pixel detectors. We also report measurements on the electron mobility, density of gap states, and on Δ, step and 1/f noise, visible light detection, and radiation damage by fast neutrons. From these measurements we calculate that pixel devices made from presently achievable a-Si:H diodes can detect minimum ionizing particles and scintillation light with adequate (>20) signal to noise when coupled to individual low-capacity, charge-sensitive amplifiers. Furthermore, extrapolation of radiation-damage measurements shows that such devices can survive in the intense background radiation at high-energy accelerators.

II. Description of the a-Si:H Diodes

Measurements were made with both 12- and 27-μm-thick, fully depleted, reverse-biased diodes. We used 12-μm n-i-p, made at Xerox, Palo Alto, and 12- and 27-μm-thick p-i-n diodes, made for us by Glasstech Solar (GSI).(2) The diodes were all deposited on glass substrates with semi-transparent chromium, palladium, or tin oxide (SnO_2) contacts. There appeared to be no significant electrical difference between the two types of 12-μm diodes. The Xerox 12-μm-thick detectors were made in a glow-discharge machine on a glass substrate covered with a conducting Cr layer. The n and p layers were deposited to a thickness ~50 nm. The thick i layer—12 μm—was deposited at a deposition rate of about 2 microns per hour which is a higher deposition rate than usually used, but still produces a-Si:H with a low dangling bond density, $< 1 \times 10^{15}/\mathrm{cm}^3$. Five mm diameter semi-transparent Cr contacts were evaporated on the 2.0-cm^2 samples.

The 12- and 27-μm GSI p-i-n detectors were deposited on a 10 × 10 cm glass substrate over a thin conducting $\mathrm{SnO_2}$ layer. The thin p and n layers, between which were sandwiched the thicker i layers, were 40-nm thick. The i layer was deposited at a temperature of 250°C and a rate of ~1 μm/h. The final detector was cut up into 2 × 2 cm squares and a thin 6.4-mm-diameter palladium contact was deposited on the top. Diode current and noise were measured as a function of reverse bias for all samples. The result of a typical measurement is shown in Fig. 1. The noise of the amplifier when loaded with a capacity equal to that of the a-Si:H sample (130 pF) and a parallel current equal to the reverse diode specific voltage is shown. The increase in noise above ~350 V may be due to partial breakdown caused by weak spots in the deposition—possibly caused by grains of dust on the substrate.(3)

III. Signal Measurements

A. Pulsed Light Signals

The objective of these measurements was to obtain the depletion-layer width from the measured signal output as a function of bias voltage. The 760-mm light has a mean-free-path in a-Si:H of ~ 100 microns, and hence the distribution of e,h pairs through the diode simulates the response of a minimum-ionizing particle. The 665-nm light has a mean-free-path <1 μm in a-Si:H. Hence, when the light is shone through the n-layer contact, the holes have to travel through the thick i layer. Alternatively, when the 665-nm light is shone through the p layer contact, the electrons produced have to travel through the thick i layer. Fig. 2 shows the corresponding plateau curves as well as those produced by the long mean-free-path 760-nm light. As expected the signal-vs-voltage curve for the 760 nm light is essentially the same when incident on the n or p contact. The electron signal approaches its maximum amplitude at about 300 V. This is also the voltage at which the hole signal starts to be observed, which shows that the depletion region is growing out from the p-type contact, towards the n layer contact where the holes are created.

Fig. 3 shows the signal response as a function of the peaking time of an RC-CR shaping amplifier from 0.2 to 9 μs for an applied voltage of 600V. The electron collection drops less than 10% at the 0.2-μs peaking time, which is consistent with our measurements of the electron mobility $\mu_e = 1.4$ cm^2/Vs for the GSI 27 μm p-i-n detectors, since the electron transit time $d^2/\mu_e V$ is 8.7 ns. The comparable transit time for holes which have a mobility of ~0.01 cm^2/Vs is 1.2 μs, and agrees with the hole data in Fig. 3. The measured drop of ~35% in signal amplitude for the 760-nm light when the peaking time is reduced from 3 μsec to 0.2 μsec is the expected signal drop for minimum ionizing particles—which are simulated by the almost uniform production of e,h pairs through the i layer.

B. Pulsed X-Ray Measurement

These were described in a previous paper.(4) They were undertaken to measure W, the average energy deposition required to produce one e-h. The intensity of the x-ray pulse signal was calibrated using the average value of 3 xtal Si, fully-depleted diodes ranging in thickness from 160-220 microns. Our measured value, W=6±0.2 eV, is consistent with an empirical relationship between band gap and W.(5)

C. Minimum Ionizing Particle Measurement

We used a 2-MeV ^{90}Sr beta source. The experimental set-up is shown in Fig. 4a. As described in (4), we used a pulse-averaging technique to bring the signal from the incident electron above the noise of the charge-sensing amplifier when loaded with the capacity of the a-Si:H detectors. Fig. 4b shows the resultant signal from the betas well separated from the noise, for a 27-μm p-i-n diode at 300-V bias.

Fig. 5 shows plateau curves for a 12 μm n-i-p Xerox detector. These were taken with an RC-CR peaking time of 3 μsec. The signal plateau yield of 500 electrons for a detector thickness of 12-μm is consistent with our value of W = 6 eV and the known dE/dx of minimum ionizing electrons traversing a-Si:H of density $\rho = 2.3$ gm/cm^2. This turns out to be a yield of 58 electrons per μm.

Fig. 5 also shows the plateau curve of the same detector when placed at $55-60^\circ$ relative to the beta particle trajectory. The increase in signal size corresponds only to the increase in path length. There is no additional enhancement as was previously observed for more heavily ionizing particles - alphas, 1- and 2-MeV protons.(6,7) We therefore conclude that for minimum-ionizing particles there is little or no signal saturation due to charge recombination in the e-h column.

Fig. 6 shows similar plateau curves taken with a 27-μm-thick p-i-n detector made by GSI at 0° and at $55-60^\circ$.

IV. Mobility and Density of States Measurements

We have used transient photoconductivity experiments to measure the electron mobility and the density of ionized dangling bonds in some of our 12-μm (n-i-p and p-i-n) detectors. For this purpose we used a nitrogen pulsed dye laser system with a pulse duration of 5 ns at a wave length of $\lambda = 510$ nm, which has an absorption depth of less than 1 μm in a-Si:H as described by Street.(8)

In the conventional time-of-flight experiment the drift mobility is determined by measuring the transit time of the electrons, a few tens of microseconds after the application of a pulsed bias field. The pulsed bias ensures that at these short times very few of the dangling bond levels are ionized. Hence, to a good approximation, the electric field is uniform through the bulk of the i layer. The photocurrent J resulting from the applied field F is

$$J = \eta n e \mu F \tag{1}$$

where n is the number of photons absorbed, η is the carrier generation efficiency, and μ is the drift mobility of the carrier selected for transport by the polarity of the applied field. The mobility is obtained from the transit time τ,

$$\mu = d/F\tau, \tag{2}$$

where d is the sample thickness. For nondispersive transport, τ is defined as the time at which J drops by 50%, while for dispersive transport it is given as usual by the change of slope in a $\log J$-$\log t$ plot.

The dangling bond density is determined by measuring the transient photoconductivity signal from the pulsed laser on a sample with an equilibrium D.C. bias. The depletion field F depends on the distance x into the sample, so that the photocurrent is time dependent, corresponding to the drift of the charge packet down the field,

$$J(t) = \eta ne\mu F(t). \tag{3}$$

For carriers that start at $x = 0$ at time $t = 0$, x is related to t by

$$x = \int_0^t \mu F(t')dt'. \tag{4}$$

$F(x)$ can therefore be obtained directly from measurement of $J(t)$ using Eq. (4), provided that $F(t)$ and the mobility are known. Since the current is proportional to the field, $F(t)$ can be found by comparing ~~the current~~ to that obtained for a known applied field and using Eq. (1) as in the TOF experiment. In this way, the number of carriers ηn does not need to be known, provided it is the same for the two experiments. The photocurrent is analyzed to give the shape of the depletion layer, from which the density of states is deduced. Results from a 12-μm n-i-p (Xerox) detector are shown in Fig. 7. The top part (Fig. 7a) shows a pulsed bias transit time induced signal. Fig. 7b shows the D.C. bias results. Our measurements show that the electron mobility is ~1.1 cm^2/Vs for the n-i-p (Xerox) detector. The 12-μm p-i-n (GSI) detector gave $\mu_e \sim 1.4 cm^2/Vs$. The corresponding densities of states are $\sim 7 \times 10^{14}/cm^3$ [n-i-p, Xerox] and $\sim 5 \times 10^{14}/cm^3$ [p-i-n, GSI].

V. Radiation Damage

In present and future colliding beam accelerators tracking and calorimeter detectors will be exposed to many-megarad particle and photon fluences. We have previously reported$^{(7)}$ measurements of damage to an a-Si:H detector sample after exposure to a fission-spectrum neutron fluence of 10^{13} cm^{-2}. We have now made more detailed measurements using samples of the 12-μm detectors, and exposing them up to much higher fluences in the exposure room of the Berkeley Research Reactor. The detectors were exposed in steps, beginning at 5×10^{12} n/cm^2 and increasing up to a final exposure of 4×10^{14} n/cm^2. After each exposure leakage current and noise measurements were made, and the ability to detect 6-MeV α particles was checked. After the final exposure and measurements, the detectors were annealed in air at 180°C for two hours, and the leakage and noise were again measured. Fig. 8 shows the leakage current (a) and the α signals and noise (b) as a function of the detector bias. After the full exposure, but before annealing, the α signal decreased by ~20% and the leakage increased by a factor of 10 at low bias, but after annealing the detector performance was indistinguishable from that before irradiation.

A comparison xtal Si detector exposed to these fast neutron fluences ceased operation after 3×10^{12} n/cm^2 exposure. Thin film transistors made from a-Si:H have been subjected to up to 10 megarad photon fluences$^{(9)}$ and shown to have minimal changes in their g_m characteristics.

VI. Pixel Detectors for Minimum Ionizing Particles

In the preceding sections we have shown that minimum ionizing electrons produce ~58 e-h pairs per micron of a-Si:H layers. For a 27-μm layer the collected charge with a 3-μsec peaking time charge-sensitive amplifier is 1300 electrons. This is below the noise level of a conventional amp loaded with a detector capacity of 130 pf of the 6.4-mm diameter contact of the 27-μm detector.

The noise of the detector-amplifier system can be reduced to <100 electrons as in CCD devices, where the capacity of each element and its integrated circuit amplifier is less than 0.1 pf. Hence, by making a pixel detector with pixel elements 100 μm × 100 μm and using integrated individual low-capacity, charge-sensitive amplifiers attached to each pixel, the S/N can be increased to the point that minimum ionizing particles can be detected unambiguously above noise. Schemes of this sort using xtal Si detector layers 200–300 μm thick bonded to xtal Si integrated circuit chips are under development by various high energy physics groups(1) planning future detectors for high intensity colliding beam accelerators including the proposed Superconducting Super Collider (SSC).

In order to estimate the S/N of a-Si:H pixel detectors of a given thickness and capacity, we have to measure the various noise contributions. The a-Si:H generates 1/f noise basically, since the random nature of e(or h) falling into and being released from shallow traps in the band tails generates this kind of noise. This 1/f contribution is proportional to the volume of the a-Si:H.(10)

Following Goulding and Landis,(11) we calculated this 1/f noise contribution by decomposing the measured noise of the amplifier-detector combination as a function of peaking time into three components—delta, step, and 1/f noise—by least square fitting. 1/f noise is taken to be independent of peaking time in the range of our interest. The value of 1/f noise that we obtained, as shown in Fig. 9 is 450 electrons for a 12-μm-thick sample with contact area 0.32 cm^2. This is in agreement with the value measured in Fig. 1 where at low voltages the noise difference between the detector and the capacity value can be attributed to 1/f noise.

The Δ noise for a detector amplifier combination is given by the following equation$^{(11)}$

$$\overline{E_\Delta^2} = \frac{kTC^2e^2}{2q^2\tau_0 g_m}$$

where C is the combined capacitance of the detector and the input stage of the FET, g_m is the transconductance of the FET, τ_0 is the RC-CR peaking time, q is the electron charge, $e = 2.718\ldots$, and k is the Boltzmann constant. We assume the equivalent value of input impedance to be $\sim 1/g_m$.

The step noise arises from the reverse and leakage currents of the diode, denoted as I. This is $\overline{E_s^2} = \frac{Ie^2\tau_0}{4q}$. To estimate the noise in a pixel device we will assume that the input capacity and g_m of the charge sensitive individual amplifier are C = 0.1 pf and $g_m = 5$ μA/V.

In Table I below we summarize the expected noise for two different pixel sizes: 1) 100 × 100 μm and 2) 300 × 300 μm and for detector thicknesses 25, 50, and 75 microns. Assumed parameters are also shown below the table.

TABLE I

	Detector Thickness		
	25 μm	50 μm	75 μm
A. 100 × 100 μm Pixel			
C_{DET} (pF)	0.042	0.021	0.014
$C_{DET} + C_{AMP}$ (pF)	0.14	0.12	0.11
1/f Noise (electrons)	0.41	0.82	1.2
Δ Noise (electrons)	48	41	37
Step Noise (electrons)	24	24	24
Total Noise (electrons)	54	46	44
S/N	23	54	85
B. 300 × 300 μm Pixel			
C_{DET} (pF)	0.38	0.19	0.13
$C_{DET} + C_{AMP}$ (pF)	0.48	0.29	0.23
1/f Noise (electrons)	3.7	7.4	11
Δ Noise (electrons)	130	99	78
Step Noise (electrons)	72	72	72
Total Noise (electrons)	150	120	110
S/N	8	21	34

Assumed parameters: $g_m = 5\ \mu A/V$
$C_{AMP} = 0.1$ pF
detector leakage current density $= 5 \times 10^{-7}\ A/cm^2$
peaking time $= 1\ \mu$sec
1/f Noise $= 1.6 \times 10^6$ electrons/cm^3
Signal $= 50$ electron/μm
Room temperature.

For charge-sensitive thin film amplifiers three technologies are considered: 1) a-Si:H FET, 2) polysilicon thin film FET, or 3) silicon on insulator (SOI) thin film single-crystal FET. Various properties of FET's produced by these technologies are listed below in Table II.

TABLE II

FET Type	e Mobility	g_m	Frequency	Radiation Hardness
a-Si:H	1-1.5 cm^2/Vs	$\sim$5 $\mu A/V$	$\sim$5 MHz	Excellent
Polysilicon	100–200 cm^2/Vs	100–150 $\mu A/V$	$\sim$50 MHz	Unknown
Crystalline (SOI)	$\sim$1000 $cm^2/Vsec$	$\sim$1 mA/V	$\sim$500 MHz	Poor

The a-Si:H transistor technology is well developed at present. The deposition temperature ($\sim$ 250°C) is compatible with most conventionally used substrates including polyimide plastic. For our purposes the distributed electronics can be deposited on the substrate or on top of the detector layer.

Polysilicon transistor technology is undergoing rapid development and thin-film transistors (TFT) are already in use in liquid-crystal displays. High-quality devices with an electron mobility of 100 cm^2/Vs can be made with high-temperature processing ($\sim$ 900°C). This temperature is not compatible with a glass substrate, but can be used with quartz. Lower-temperature processing requires a deposited dielectric and, at present, results in TFT's with a lower mobility. For the pixel readout the transistor layer would have to be deposited first and the detector layer deposited over it at the usual 250°C temperature.

Note from Table I that the largest contribution to the noise comes from the Δ component, which is proportional to $\sqrt{1/g_m}$. Hence, if we use polysilicon FET with $g_m \sim 150\mu$ A/V(12) we can expect the Δ noise contribution to be $\sim$5 times smaller. The step noise can be decreased by 2–3 if carbon is deposited in the blocking p layer, since this process decreases reverse current by a factor of 5–10.(13) The 1/f noise might increase due to the random nature of the electron transitions through the polycrystal boundaries.

The SOI [silicon-on-insulator] technology has been under development for ~5 years.(14) Because of its higher crystallization temperature (900–1000°C) and more difficult processing, it is more costly and would be used only if the a-Si:H or the polysilicon electronics were inadequate for the pixel readout.

There has been very little information up to this time on noise characteristics for FET's produced by any of these three technologies.

The signal amplitude can be increased by the simple expedient of depositing the pixel on a ridged substrate. With 60° ridges, the signal increase is $1/\cos 60° = 2$. Thicker layers, up to 100 μm of a-Si:H with a sufficiently low density of dangling bonds in the thick i layer have been made.(15) The electric field within the sample decreases with distance at a rate determined by the fixed charge left by the ionized dangling bond electrons. Fig. 10 shows the calculated E field versus distance as a function of dangling bond density. The black circles denote the transition voltage (~1V) from full ionization to partial ionization.(6,16)

The idea of tailoring the field profile by the multilayer structure may be useful for making a substantially thicker, still fully depleted a-Si:H layer with the present number of dangling bond density ($< 5 \times 10^{14}/\text{cm}^3$). A possible 100-$\mu$m thick multilayer structure is calculated and shown in Fig. 11.

VII. Summary and Conclusions

The measurements on relatively thick layers of a-Si:H p-i-n or n-i-p detectors show that the value of W = 6 eV, and hence the corresponding charge collection produced by minimum ionizing particles, is consistent with the fact that layers up to 27 μm can be fully depleted at voltages of <12 V/μm. We believe that depletion-layer widths of 100μm or greater are achievable with the present material-deposition techniques that can produce a-Si:H deposits with dangling bond densities of $\sim 5 \times 10^{14}/\mathrm{cm}^3$—as shown by us and by others(17). By decreasing the electrical capacity of the detector and coupled charge sensitive amplifier to ~0.1 pf we have shown that S/N for minimum ionizing particle detection >20 for 25-μm-thick detectors is achievable.

One difficulty that we can anticipate in making thicker detectors is that the a-Si:H has a built-in stress. This can be minimized by changing the glow discharge deposition conditions. Suitable compromise deposition conditions that produce a reasonable compromise among internal stress, low density of dangling bonds, and also moderately high deposition rates have been explored.(18)

In conclusion, we have shown that a-Si:H glow discharge deposits can be made thick enough so that small-area pixel or strip devices can detect minimum ionization particles adequately.

Acknowledgments

We would like to express our appreciation to C. C. Tsai and R. Thompson, of Xerox PARC, for making the samples. We also thank A. Madan and P. Bhat, of GSI, for making thicker samples. We are grateful also to K. Lee and B. Jarrett of Lawrence Berkeley Laboratory for their helpful discussions. We would especially like to express our appreciation to Fred Goulding from whom we have sought and received valuable suggestions throughout the course of this work. This work was supported by the Director, Office of Energy Research, Office of High Energy and Nuclear Physics, Division of High Energy Physics of the U. S. Department of Energy under contract #DE-AC03-76SF00098.

REFERENCES

1. LBL–U. of Hawaii–Stanford (S. Parker et al). J. Kemmer (Tech. University of Munich), C. Demerall (Rutherford Appleton Lab), unpublished.

2. Glasstech Solar, Inc.(GSI), Wheatridge, Colorado.

3. Private communication, A. Madan, GSI, (1988).

4. S. Kaplan, I. Fujieda, V. Perez-Mendez, S. Quereshi, W. Ward and R. A. Street, *Proceedings of The London Conference on Position-Sensitive Detectors* September 1987, LBL-23961, to be published in NIM.

5. C. R. Klein, J. App. Phys. *39*, 2029 (1968).

6. V. Perez-Mendez, J. Morel, S. N. Kaplan, and R. A. Street, Nucl. Instr. and Method *A252*, 478 (1986).

7. V. Perez-Mendez, S. N. Kaplan, W. Ward, S. Qureshi, and R. A. Street, Nucl. Instr. and Method *A260*, 195 (1987).

8. R. Street, Phys. Rev. B*27*, 4924 (1983).

9. I. D. French, A. J. Snell, and P. G. LeComber, Appl. Physics *A31*, 19 (1983).

10. F. Z. Bathael and J. C. Anderson, Phil. Mag. *B55*, 87 (1987).

11. F. Goulding and D. Landis, IEEE Trans. Nucl. Sci. *NS-29*, 1125 (1982).

12. S. Seki, T. Unagami, and B. Tsujiyama, *Proc. 16th Conference on Solid State Devices and Materials*, Kobe, 1984, p. 563.

13. S. Kaneko, F. Okumura, M. Sakamoto, H. Uchida and Y. Kajiwara, SPIE Vol. 617

Amorphous Semiconductors for Microelectronics , 127, (1986).

14. H. W. Lam and M. J. Thompson, *Comparison of Thin Film Transistor and SOI Technologies*, Materials Research Society Symposia Proceedings (New York: North Holland, 1984) vol. 33.

15. M. Favre, H. Curtins, and A. V. Shah, J. Non-Cryst. Solids *97*, 731 (1987).

16. J. D. Cohen, *Semiconductors and Semi-Metals* (New York: Academic Press, 1984), Vol. 21, part C.

17. S. Tsuda, T. Takahama, M. Isomura, H. Tarui, Y. Nakashima, Y. Hishikawa, N. Nakamura, T. Matsuoka, H. Nishiwaki, S. Nakano, M. Ohnishi, and Y. Kuwano, Jpn. J. Appl. Phys. *26*, 33 (1987).

18. H. Curtins, W. Wyrsch, A. V. Shah, Electron. Lett. *23*, 228 (1987).

Figure Captions

Figure 1: Current and noise (FWHM) versus bias for a typical 27 μm detector. The curve marked with open squares shows the measured noise for an equivalent capacity, 130 pf, shunted by a 10 MΩ resistor that was drawing a current equal to that shown in the top curve.

Figure 2: Voltage plateau curves for 760- and 665-nm light pulses. In both cases the light pulses were less than 100 ns wide, and the amplifier peaking time was 9 μs.

Figure 3: Output signal vs. peaking time for 665 nm and 760 nm light pulses on 27μm at 600V bias.

Figure 4: (a) Experimental setup for ^{90}Sr electron measurements

(b) Pulse height distributions of 256-trace, signal-averaged pulses, for source in, as shown in (a), and source out with a pulser triggering the scope.

Figure 5: Signal (electrons) vs. voltage for ^{90}Sr beta's 12-μm n-i-p Xerox detector at 0° and at $55 - 60°$.

Figure 6: Signal (electrons) vs. voltage for ^{90}Sr beta's from 27-μm GSI p-i-n detector at 0° and at 55-60°.

Figure 7: Time-of-flight measurements on mobility, dangling bond density.

(a) Bias = 6V, pulsed

(b) Bias = 30V, DC.

Figure 8: Measurements on 12-μm GSI detectors exposed to 5×10^{12}–4×10^{14} fast-neutron fluences.

(a) Leakage current

(b) Pulse heights from 6 MeV α particles, and FWHM noise.

Figure 9: Δ, step and 1/f noise. The 1/f noise is given by the dashed line.

Figure 10: Calculated E field for 1500-V bias applied to a 75-μm-thick detectors, having dangling bond densities ranging from 3×10^{15} cm^{-3} down to 3×10^{14} cm^{-3}.

Figure 11: Calculated E field for 2000-V bias applied across a 100-μm p-i-n diode that has had its undoped, slightly n-type, i region partially compensated by two 5-μm p-doped layers, as shown.

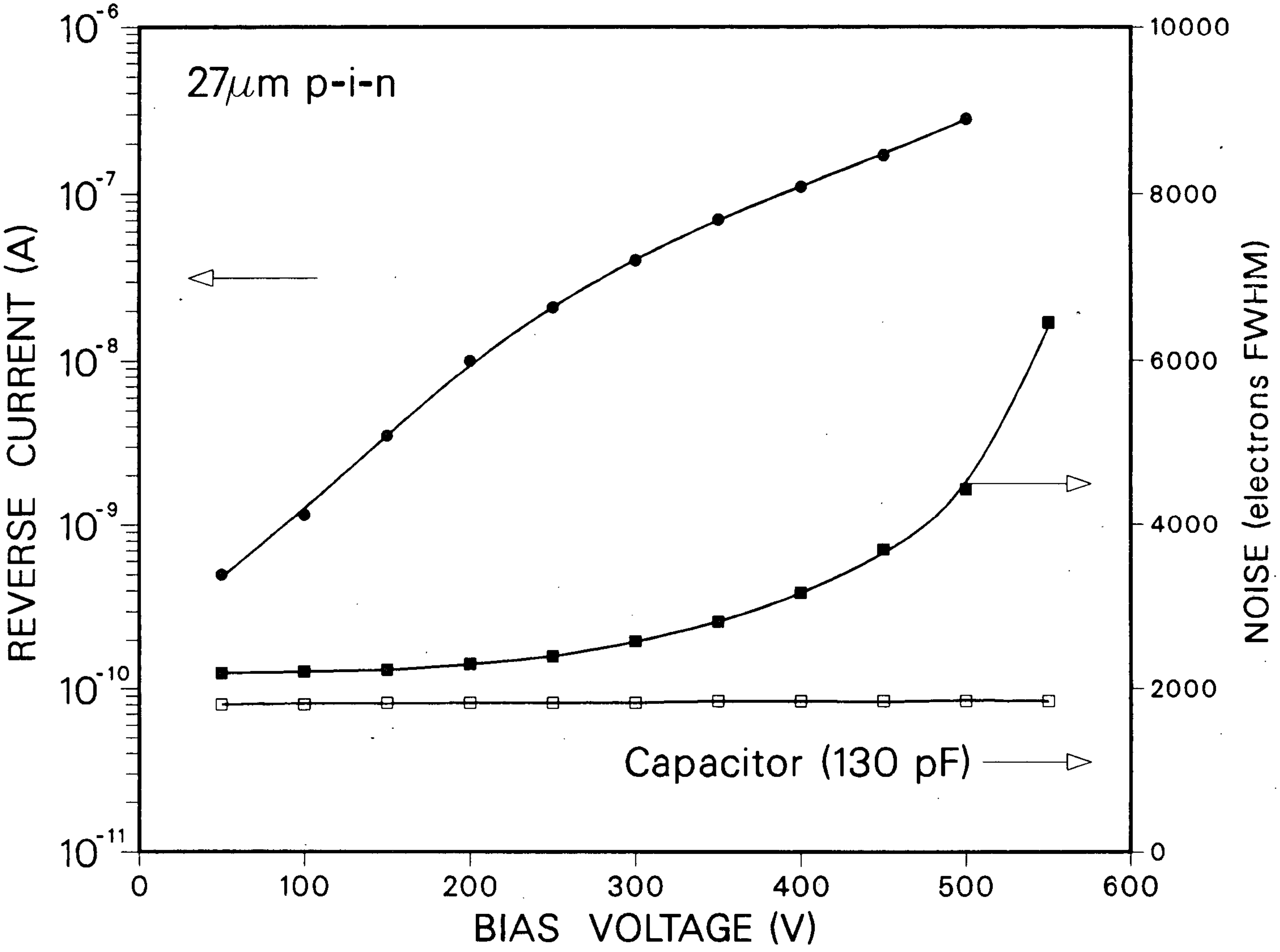

XBL 884-1253

Fig. 1

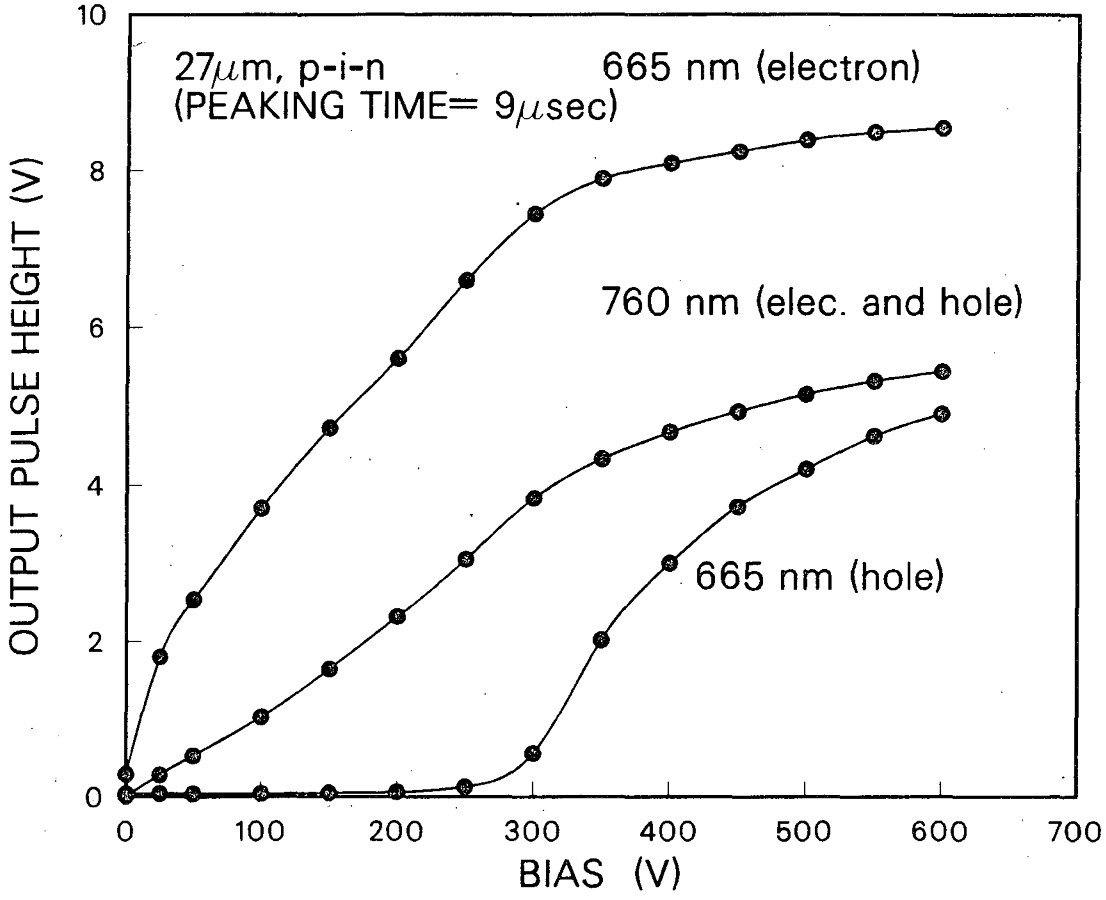

XBL 884-1254

Fig. 2

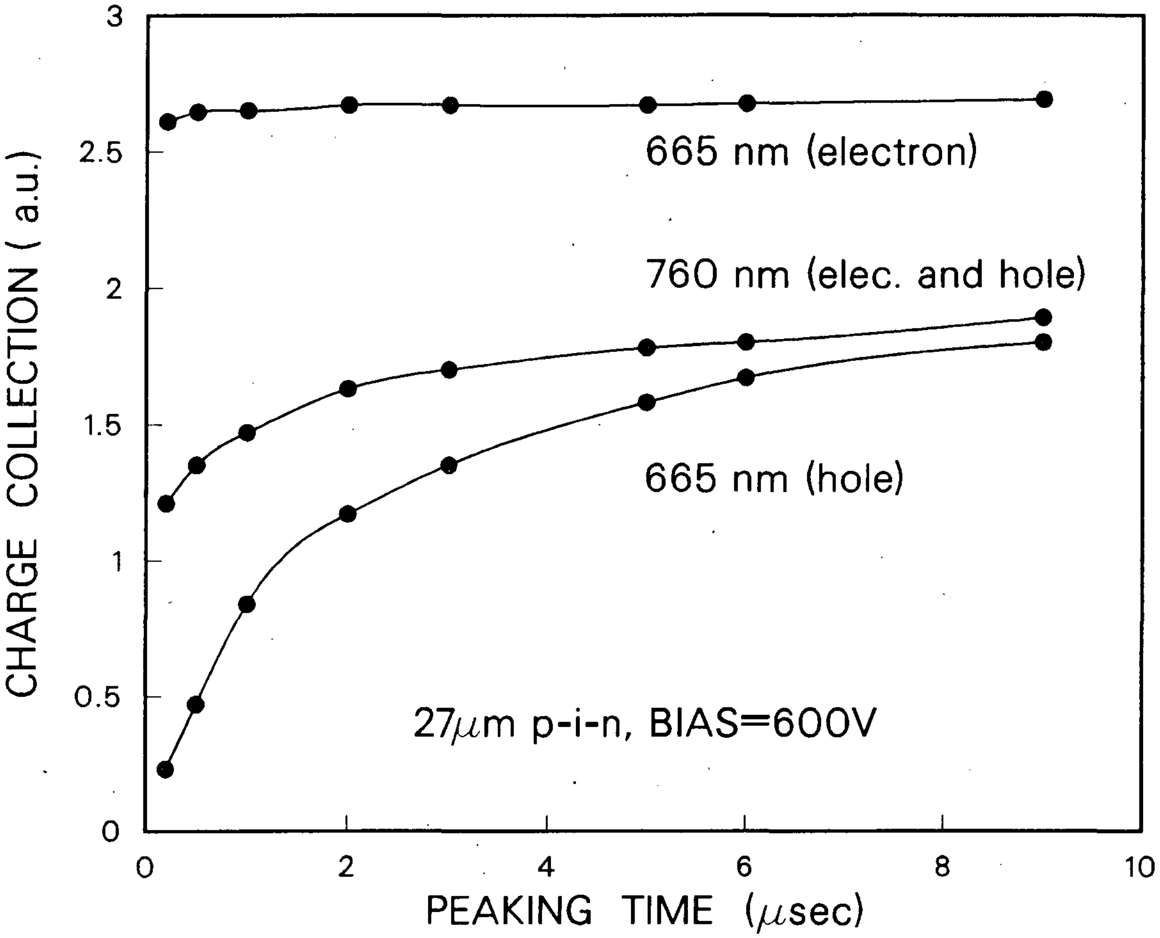

XBL 884-1255

Fig. 3

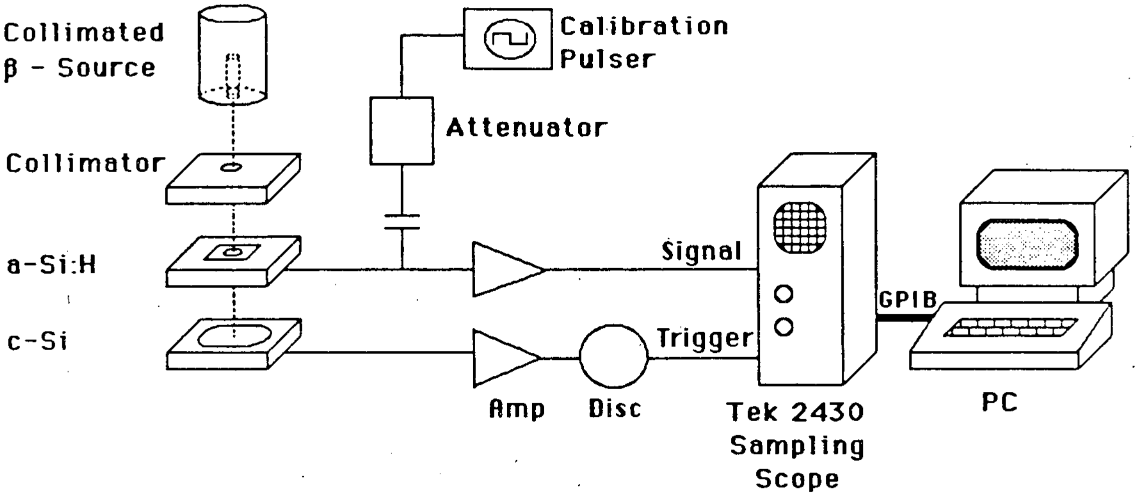

XBL 884-1256

Fig. 4a

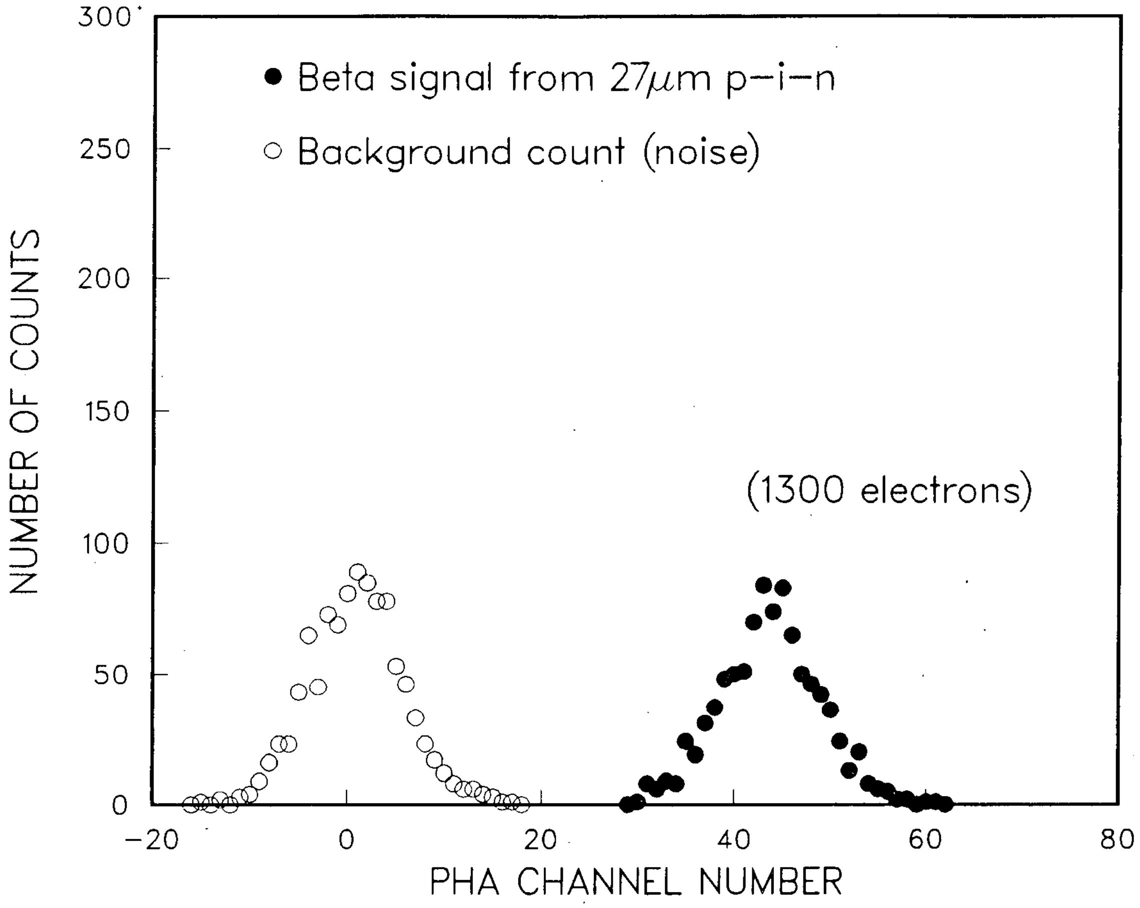

XBL 884-1257

Fig. 4b

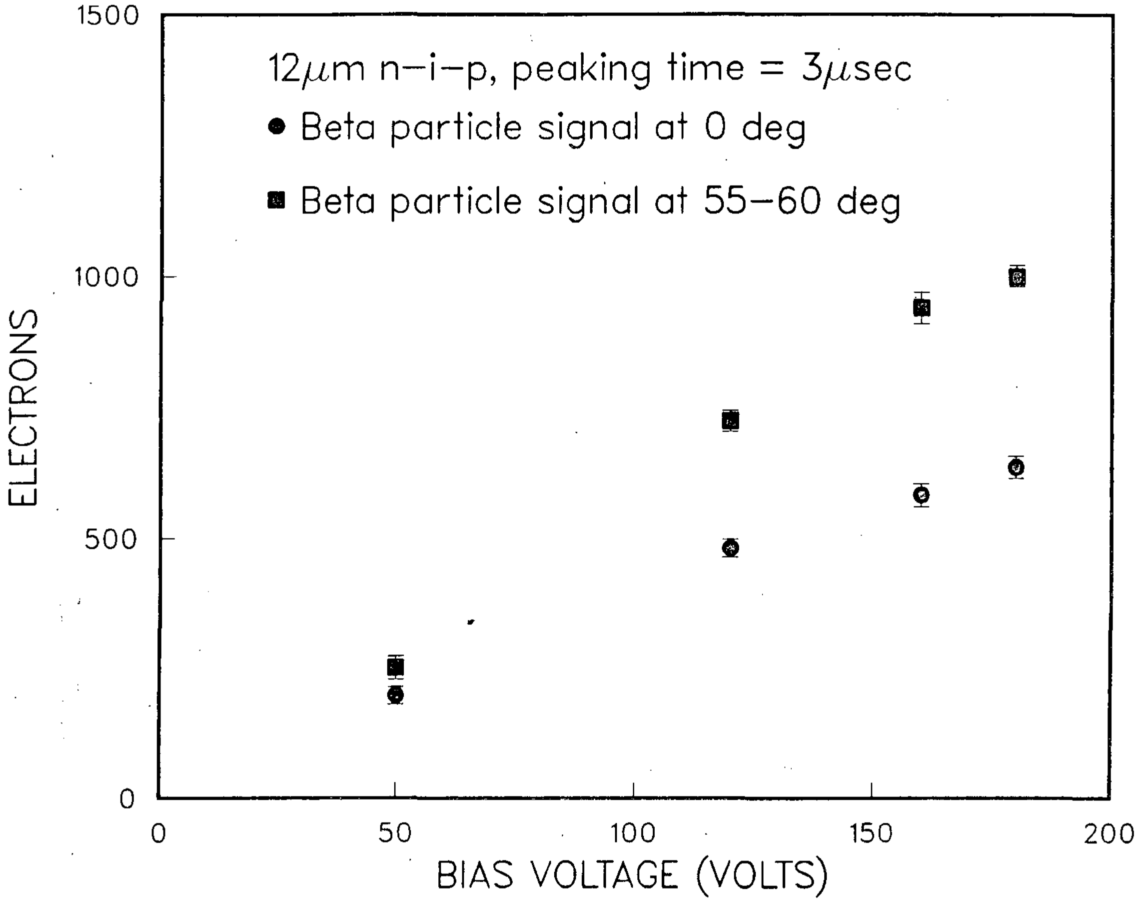

XBL 884-1258

Fig. 5

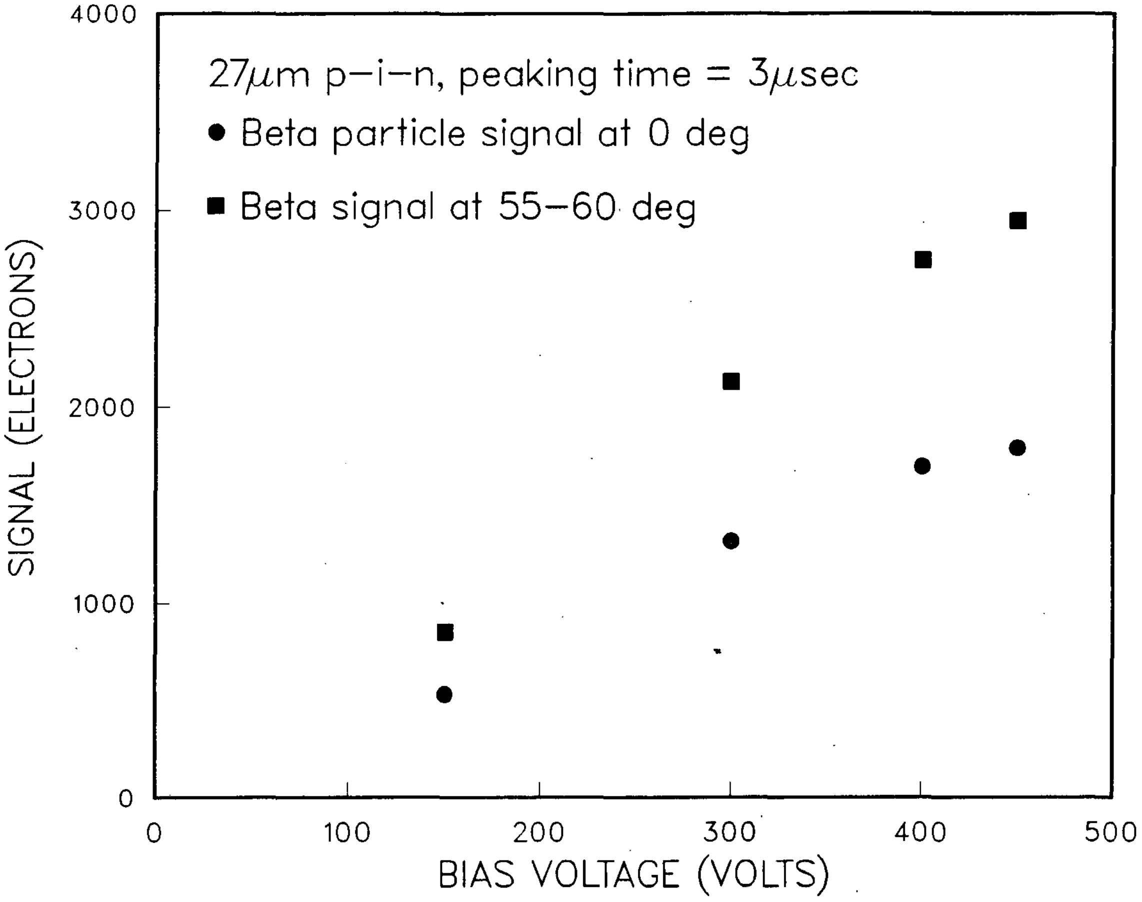

XBL 884-1259

Fig. 6

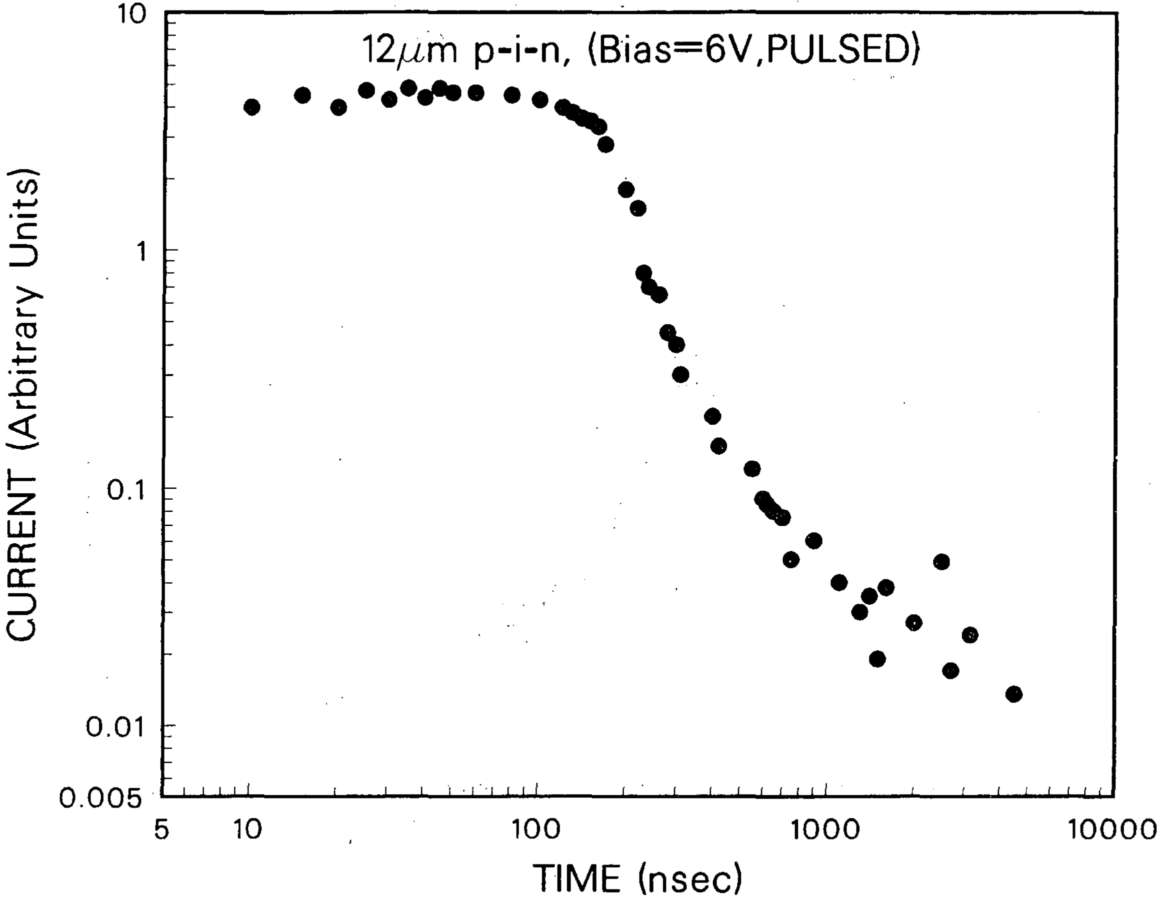

XBL 884-1260

Fig. 7a

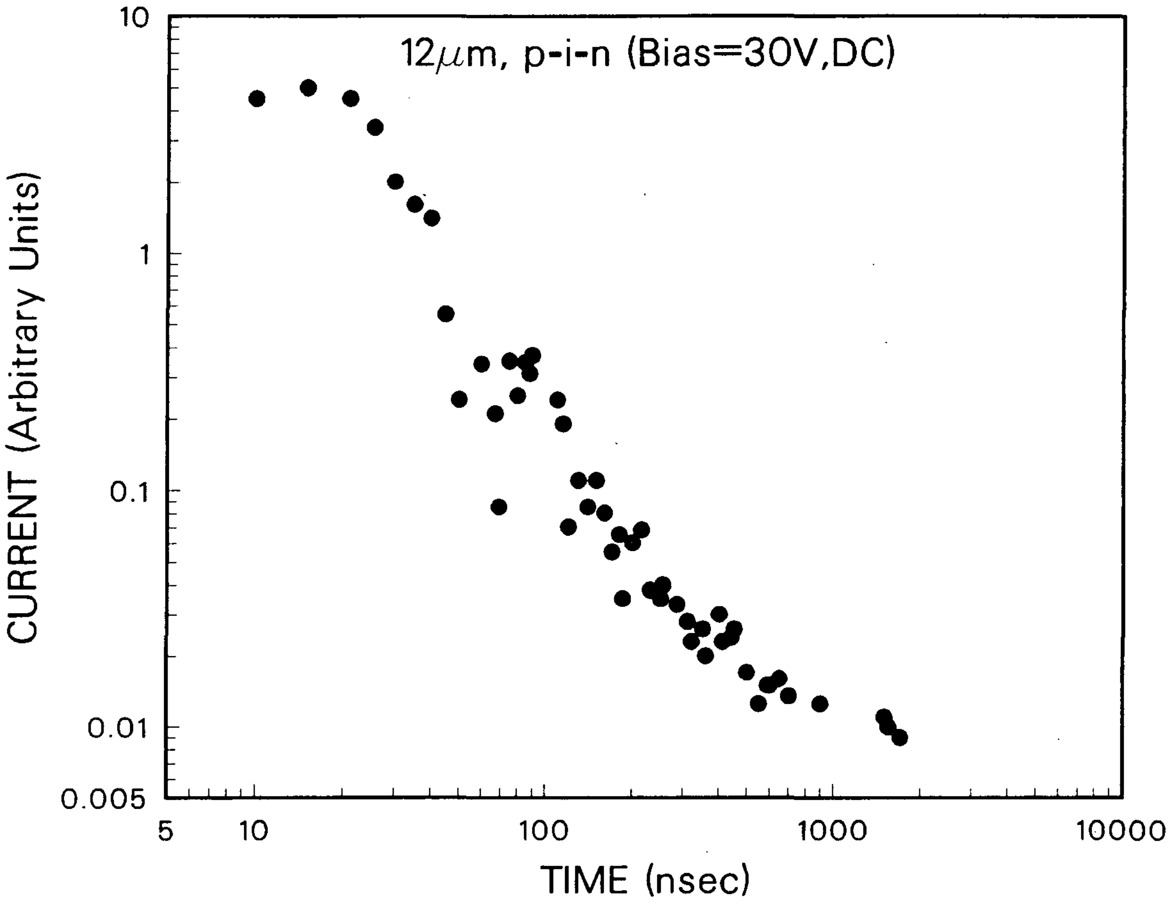

XBL 884-1261

Fig. 7b

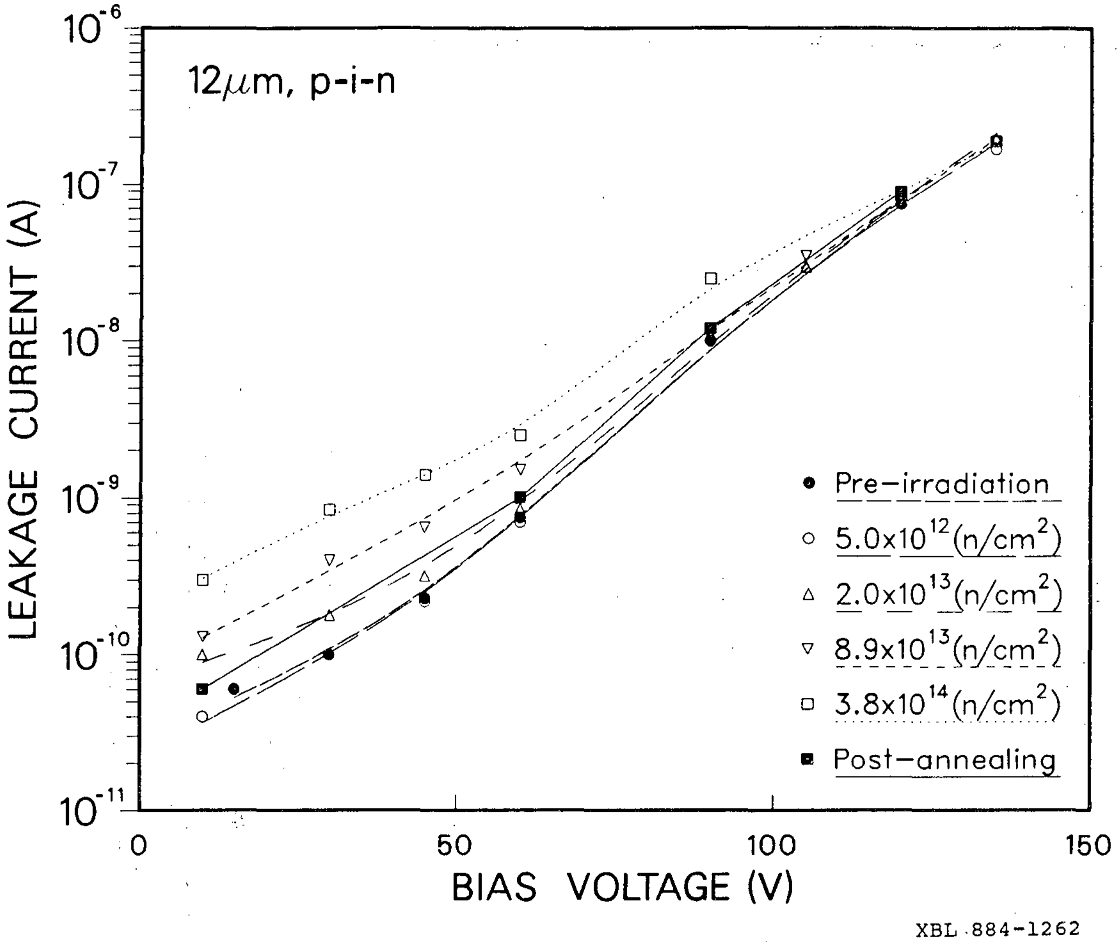
12μm, p-i-n
LEAKAGE CURRENT (A)
10^-6
10^-7
10^-8
10^-9
10^-10
10^-11
0
50
100
150
BIAS VOLTAGE (V)
● Pre−irradiation
○ 5.0x10^12(n/cm^2)
△ 2.0x10^13(n/cm^2)
▽ 8.9x10^13(n/cm^2)
□ 3.8x10^14(n/cm^2)
■ Post−annealing
XBL 884-1262

Fig. 8a

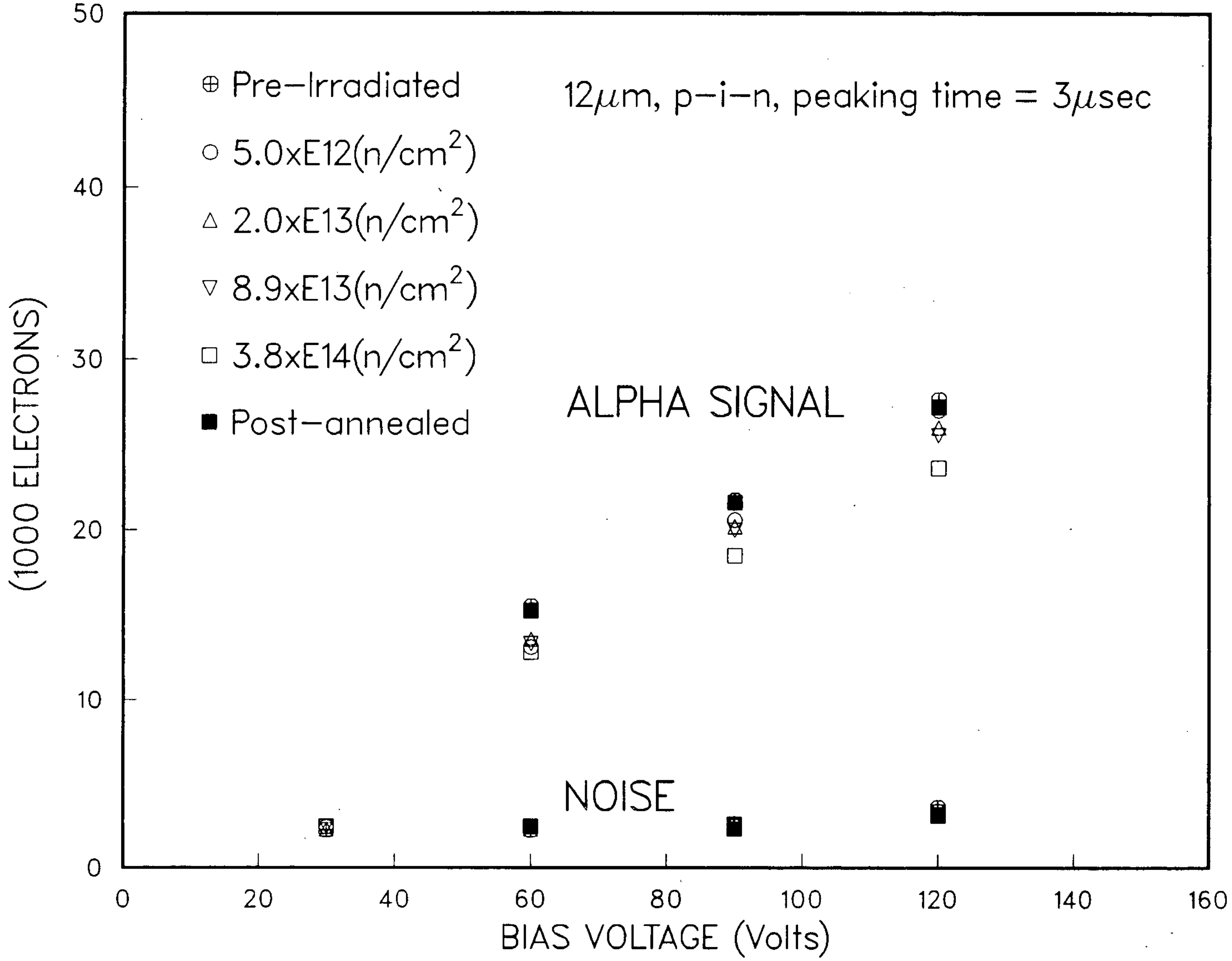

XBL 884-1263

Fig. 8b

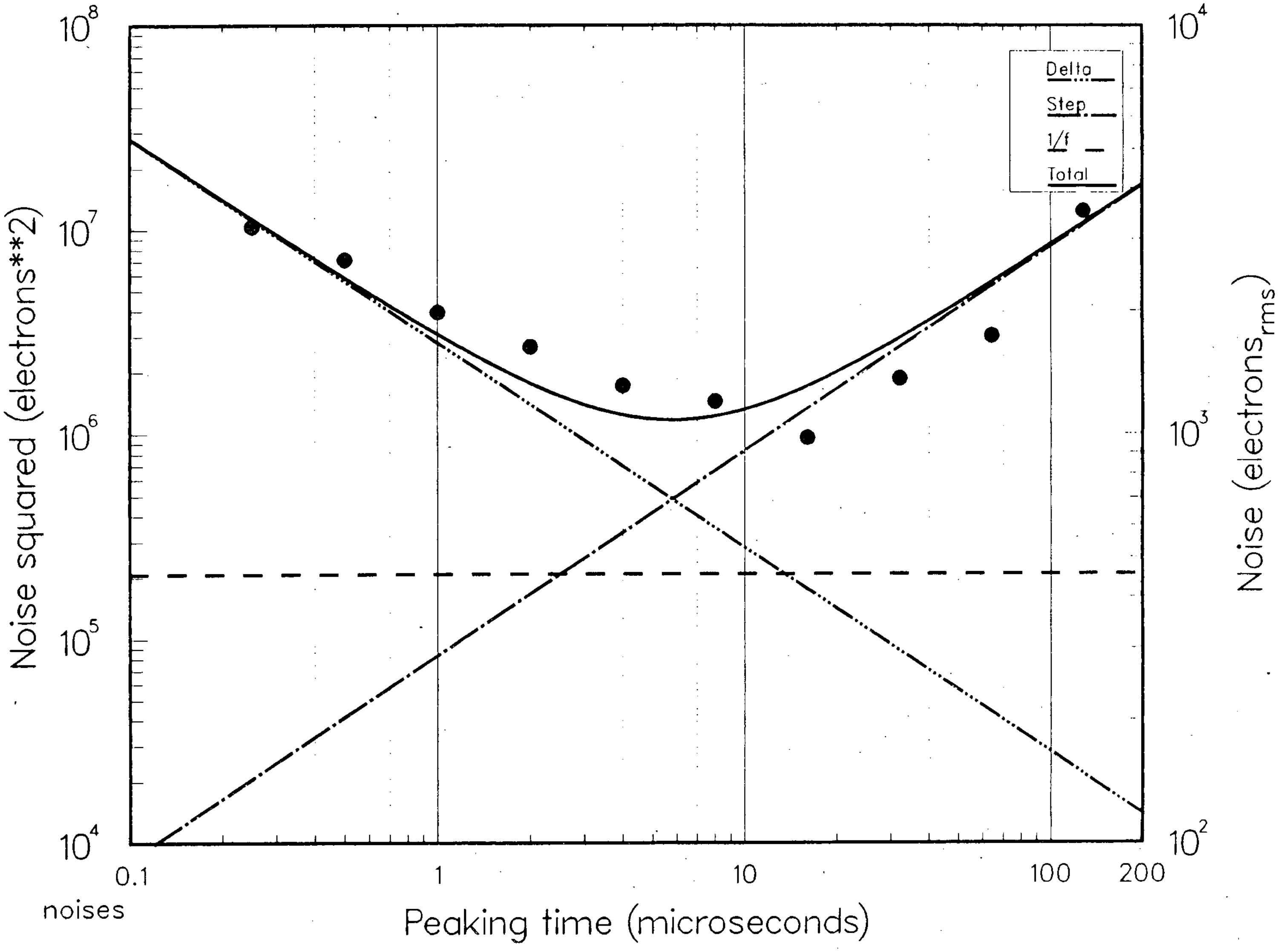

XBL 884-1264

Fig. 9

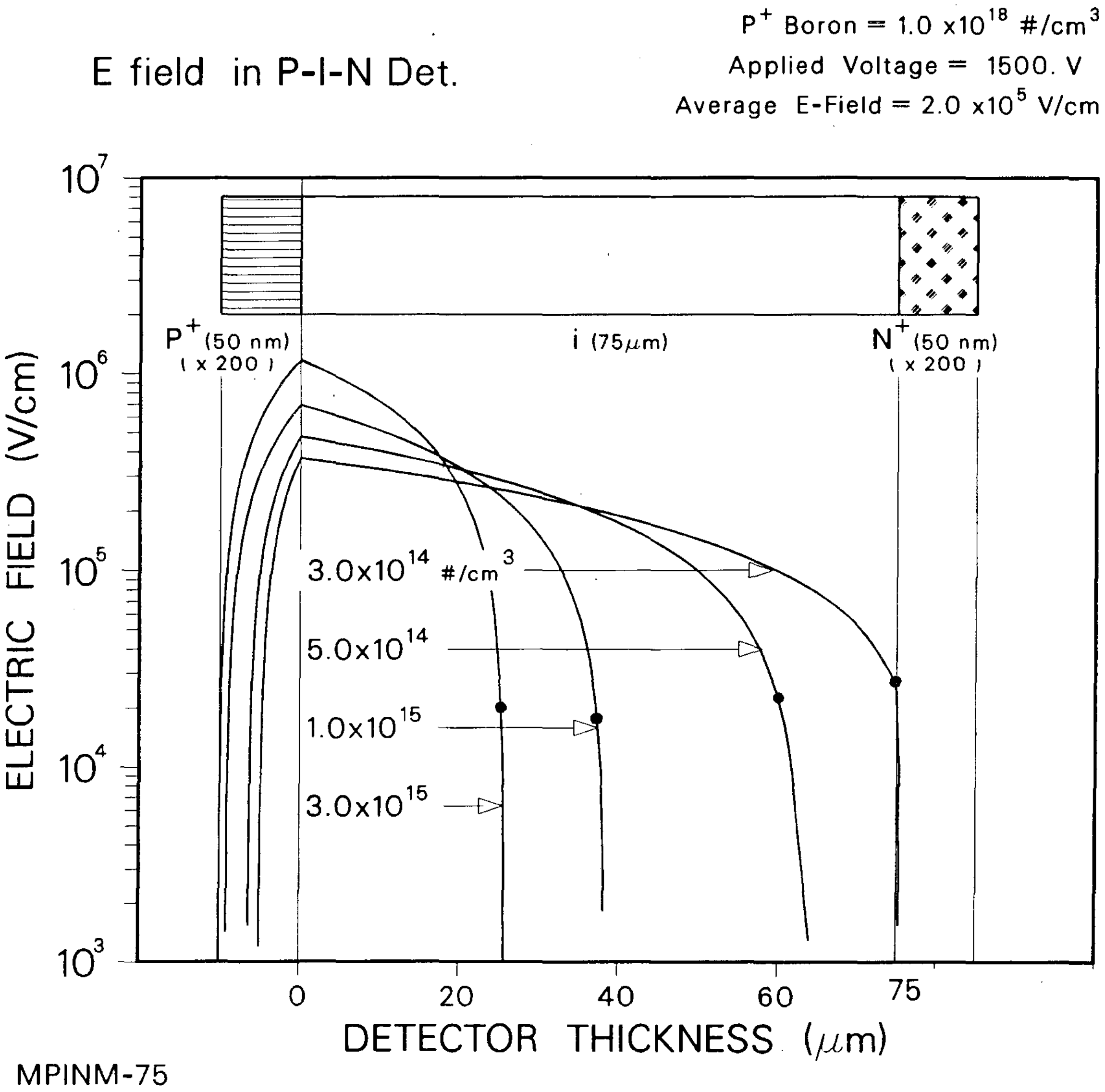
E field in P-I-N Det.
P^+ Boron = 1.0 x10^{18} #/cm^3
Applied Voltage = 1500. V
Average E-Field = 2.0 x10^5 V/cm
P^+(50 nm)
(x 200)
i (75μm)
N^+(50 nm)
(x 200)
3.0x10^{14} #/cm^3
5.0x10^{14}
1.0x10^{15}
3.0x10^{15}
ELECTRIC FIELD (V/cm)
10^7
10^6
10^5
10^4
10^3
0
20
40
60
75
DETECTOR THICKNESS (μm)
MPINM-75
XBL 884-1265

Fig. 10

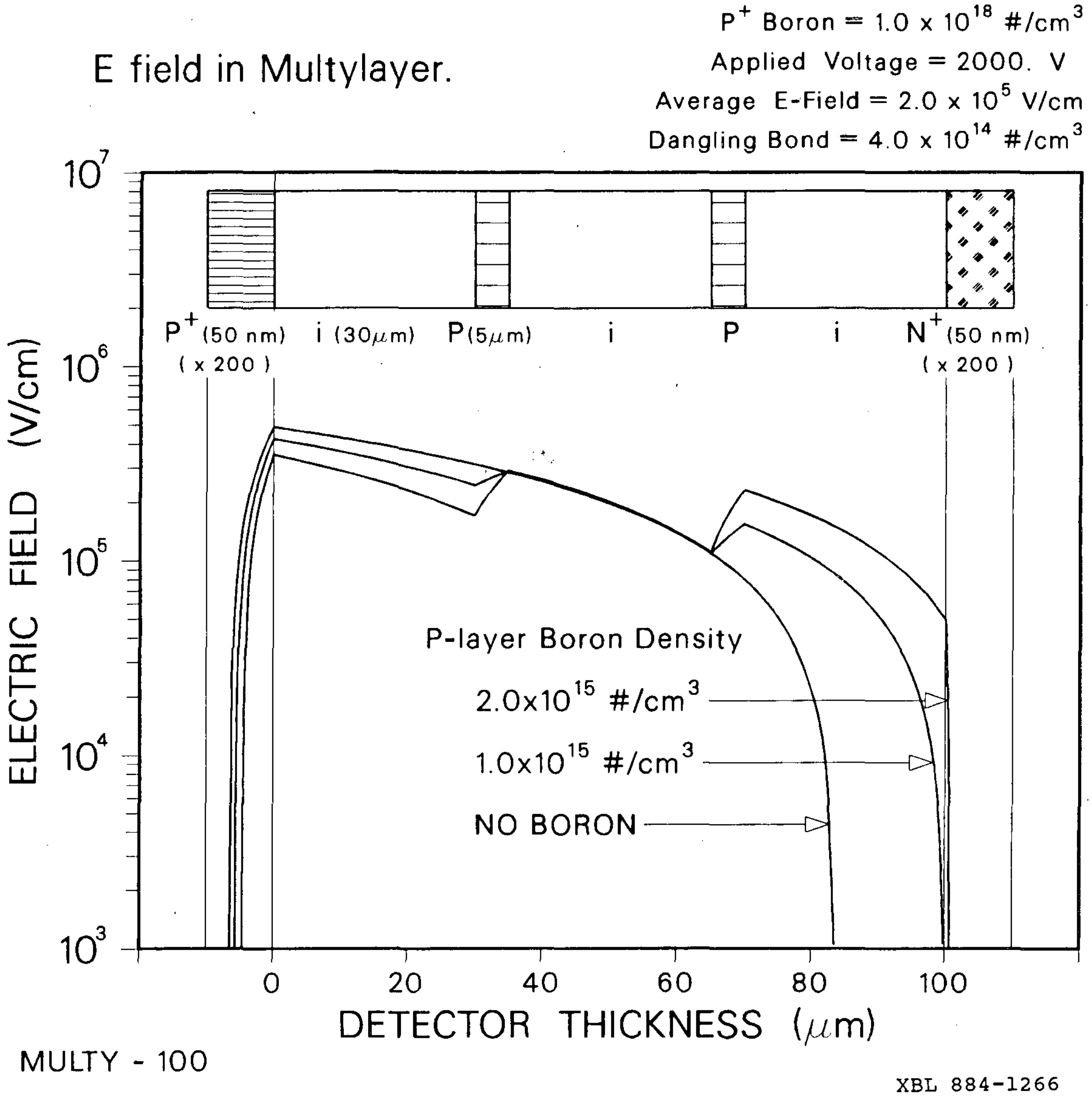
E field in Multylayer.
P$^+$ Boron = 1.0 x 10^{18} #/cm^3
Applied Voltage = 2000. V
Average E-Field = 2.0 x 10^5 V/cm
Dangling Bond = 4.0 x 10^{14} #/cm^3
P$^+$(50 nm) (x 200)
i (30μm)
P(5μm)
i
P
i
N$^+$(50 nm) (x 200)
ELECTRIC FIELD (V/cm)
10^7
10^6
10^5
10^4
10^3
P-layer Boron Density
2.0x10^{15} #/cm^3
1.0x10^{15} #/cm^3
NO BORON
0
20
40
60
80
100
DETECTOR THICKNESS (μm)
MULTY - 100
XBL 884-1266

Fig. 11

LAWRENCE BERKELEY LABORATORY
TECHNICAL INFORMATION DEPARTMENT
UNIVERSITY OF CALIFORNIA
BERKELEY, CALIFORNIA 94720